Inorganic Chemistry

Article

pubs.acs.org/IC

Highly Selective Mitochondria-Targeting Amphiphilic Silicon(IV) Phthalocyanines with Axially Ligated Rhodamine B for Photodynamic Therapy

Zhixin Zhao,[†] Pui-Shan Chan,[‡] Hongguang Li,[†] Ka-Leung Wong,[†] Ricky Ngok Shun Wong,[‡] Nai-Ki Mak,*[,‡] Jie Zhang,[†] Hoi-Lam Tam,[§] Wai-Yeung Wong,[†,∥] Daniel W. J. Kwong,*[,†] and Wai-Kwok Wong*[,†,∥]

[†]Department of Chemistry, Hong Kong Baptist University, Kowloon Tong, Hong Kong SAR

[‡]Department of Biology, Hong Kong Baptist University, Kowloon Tong, Hong Kong SAR

[§]Department of Physics, Hong Kong Baptist University, Kowloon Tong, Hong Kong SAR

[∥]Institute of Molecular Functional Materials, Areas of Excellence Schemes, University Grants Committee, Hong Kong

Supporting Information

ABSTRACT: Two axially ligated rhodamine−Si(IV)−phthalocyanine (Rh-SiPc) conjugates, bearing one and two rhodamine B, were synthesized and their linear and two-photon photophysical, subcellular localization and photocytotoxic properties were studied. These Rh-SiPc conjugates exhibited an almost exclusive mitochondrial localizing property in human nasopharyngeal carcinoma (HK-1) cells and human cervical carcinoma (HeLa) cells. Strong photocytotoxic but low dark cytotoxic properties were also observed for the two Rh-SiPc conjugates toward the HK-1 cells. Using nuclei staining method and flow cytometric DNA content analysis, apoptotic cell death was induced by these conjugates upon photoactivation. This observation is consistent with their mitochondrial localization property. The observed properties of these conjugates qualify them as promising PDT agents.

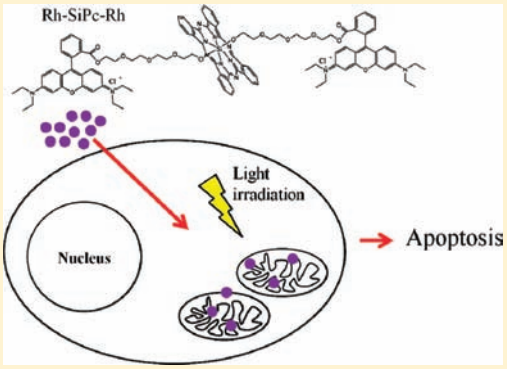

INTRODUCTION

Photodynamic therapy (PDT) has attracted increasing attention as a highly selective anticancer treatment modality where a nontoxic photosensitizer showing preferential accumulation in tumor tissue or its vasculature when administered inside the body is activated by the tumor-targeted photoirradiation at a specific wavelength to produce cytotoxic reactive oxygen species (ROS), principally singlet oxygen ($^1O_2$), which then kills the tumor cells.[1,2] An ideal anticancer PDT agent should possess the following properties: (1) minimal dark cytotoxicity, (2) relatively high $^1O_2$ quantum yield, (3) preferential uptake by target tissues, (4) strong absorption at longer wavelengths, that is, $\lambda > 650$ nm, where absorption by biomolecules, such as hemoglobin, is minimal, (5) high chemical stability, and (6) rapid clearance from normal tissues.[3] As singlet oxygen is believed to be the principal cytotoxic agent, its short reactive range (0.01−0.02 μm) in biological systems[4] is an important factor to consider in designing an efficacious PDT agent. To overcome the short reactive ranges of $^1O_2$ and other ROS, photosensitizer needs to closely localize to the targets that can effectively trigger cell death. Among the intracellular targets that have been shown to cause cell death, mitochondrion is considered quite appealing as it can cause cell death by apoptosis, which is a programmed shutdown of the cell machinery with all its components recycled without eliciting any undesirable inflammatory responses often seen in conventional chemotherapy.[5] In this work, we report the synthesis of a mitochondria-targeting PDT agent by covalently connecting a well-known mitochondria-targeting agent, namely, rhodamine B (Rh B), to a tumor-localizing photosensitizer, namely, phthalocyanine (*Pc*), and evaluated its subcellular localization, one- and two-photon PDT properties in several cancer and noncancer cell models.

This design is based on the fact that positively charged rhodamine, such as Rh B and rhodamine 123,[6] accumulates specifically in the mitochondria of living cells and has been used as probes to measure and monitor mitochondrial membrane potential in bioassays.[7] On the other hand, *Pc* is a class of photosensitizers that absorbs strongly in the tissue-penetrating spectral window of 650−800 nm and has been extensively studied as a potential PDT agent due to its tumor-localizing properties.[3,8] Since most phthalocyanines are insoluble and tend to aggregate in aqueous media, they have to be encapsulated in liposomes,[9] polymeric micelles[10] or nanoparticles[11] before their administration into test animals or cells. The aqueous solubility of *Pc* can be improved by introduction of hydrophilic substituents, such as sulfonate,[12] carboxylate,[13] *N*-methylpyridinium,[14] and polyethylene glycol (PEG),[15] in the

Received: May 31, 2011
Published: December 22, 2011

macrocyclic ring. Axial ligation of hydrophilic or amphiphilic groups in metallophthalocyanines, including silicon(IV) phthalocyanine (SiPc), which is currently under clinical trial,[8] is another approach to increase water solubility and reduce aggregation in aqueous media.[16] Recently, the synthesis and PDT activity of the hydrophobic monohydroxy trisphenylporphyrin (TPP-OH) tethered to Rh B via a saturated hydrocarbon linker has been reported.[17] Enhanced (>5-fold) photocytotoxicity, relative to its components (i.e., TPP-OH and Rh B), and preferential accumulation at mitochondria were observed for this conjugate. Similar conjugates of sulfono- and carboxy-substituted phthalocyanines with rhodamines have also been synthesized[18] and their efficient intramolecular energy transfer (from Rh to *Pc*) studied as well.[19] In our design, Rh B, instead of connecting to the macrocyclic ring as peripheral substituents as in previous works,[17−19] is axially connected to SiPc via a polyether linkage to form two SiPc-Rh B conjugates, **3** and **2**, possessing one and two Rh B moieties, respectively. This axial ligation design can reduce *Pc* aggregation, thereby increasing its excited state lifetimes[20] and improving its cellular uptake and imaging properties. The synthesis, linear and two-photon photophysical, subcellular localization, and in vitro PDT activity of these conjugates are reported herein.

EXPERIMENTAL SECTION

General Remarks. All reactions were carried out in a dry nitrogen atmosphere. Solvents were dried by standard procedures, distilled, and deaerated prior to use. All chemicals were obtained from Aldrich Chemical Co. and, where appropriate, degassed before use. NMR spectra were recorded with a Varian INOVA 400 NMR spectrometer. High-resolution matrix assisted laser desorption/ionization time-of-flight (MALDI-TOF) mass spectra were recorded with a Bruker Autoflex MALDI-TOF mass spectrometer. Electronic absorption spectra in the UV/vis region were recorded with a Varian Cary 100 UV/vis spectrophotometer. Steady-state visible fluorescence and photoluminescence excitation spectra were recorded with a Photon Technology International (PTI) Alphascan spectrofluorimeter and singlet-oxygen near-IR (NIR) emission spectra were recorded directly by its phosphorescence emission at 1270 nm with an InGaAs detector, using H_2TPP ($\Phi_\Delta = 0.55 \pm 0.11$)[21] as the reference compound. The filter was LG-697-F from Corion Company. Infrared spectra (KBr pellets) were recorded with a Nicolet Magna 550 FTIR spectrometer. All measurements were performed at ambient temperature (20 ± 2 °C) and pressure. The UV/vis absorption and NIR emission spectra of all solution samples were measured in a 10 mm quartz cell.

Cell Culture. Human nasopharyngeal carcinoma (HK-1) cells were cultured in RPMI-1640 medium (Gibco) supplemented with 10% fetal bovine serum (Gibco) and antibiotics (penicillin 50 U/mL; streptomycin 50 μg/mL). Human cervical carcinoma (HeLa) cells were maintained in an RMPI 1640 medium supplemented with 10% fetal bovine serum (FBS) and 1% penicillin and streptomycin. Cells were incubated at 37 °C in a humidified incubator with 5% CO_2. Culture medium in each dish was changed prior to exposure to the test compounds. Stock solutions of the test compounds (1 mM) were prepared in DMSO and stored in dark at room temperature. These compounds, when used in the imaging and bioassay experiments involving cultured cells, were diluted with the corresponding culture media to appropriate concentrations.

Confocal Microscopic Imaging of Rh-SiPc Conjugates. HK-1 cells (1×10^5) were seeded onto coverslip in 35-mm culture dishes for overnight. The cells were initially incubated with Rh-SiPc-Rh (**2**, 50 nM), Rh-SiPc (**3**, 50 nM), Rh B (1 μM) or C-SiPc-C_7 (**4**, 1 μM) for 30 min in dark. The cells were then washed and stained with 100 nM mitochondria-specific probe, Mito Tracker Green FM dye M7514, lysosomes-specific probe Lyso Tracker Green DND-26 L7526, Golgi-specific probe BODIPY FL C5-ceramide complexed to BSA B-22656 and the endoplasmic reticulum probe ER Tracker Blue−White DPX dye E12353 (Invitrogen) for 30 min. The emitted fluorescent signals of **2**, **3**, Rh B, **4** and the organelle-specific probes were examined using the (Olympus) FV1000 confocal microscope equipped with a spectral detection system. A diode laser line at 405 nm was used for excitation of the ER Tracker. An argon-ion laser line at 488 nm was used for the excitation of Mito Tracker, Lyso Tracker and Golgi Tracker. A helium−neon laser line at 543 nm was used for the excitation of **2**, **3**, Rh B and **4**. Emission signals at 425−475 nm (ER Tracker), 500−530 nm (Mito, Lyso and Golgi Trackers), 620−720 nm (**2** and **3**), 560−660 nm (Rh B) and 630−710 nm (**4**) were collected. A 60x oil immersion objective and pinhole size of 110 μm was used for image capturing. Images were processed and analyzed using the FV10-ASW software (Olympus).

Photocytotoxicity Assay. HK-1 cells (2×10^4/well) were incubated in wells of 96-well plate for overnight. The cells were treated with **2** (100 nM), **3** (100 nM), Rh B (100 nM), or **4** (100 nM) for 6 h in dark. The culture medium was then replaced with fresh medium and the cells were exposed to yellow light (1−4 J/cm^2) produced from a 400 W tungsten lamp fitted with a heat-isolation filter and a 500 nm long-pass filter. The fluence rate was 4 mW/cm^2. Cells viability was determined by the MTT reduction assay at 24 h post-PDT.[22] The cell monolayers were rinsed twice with phosphate-buffered saline (PBS) and then incubated with 250 μg/mL MTT solution at 37 °C for 3 h. The formazan crystal formed was dissolved in DMSO and the absorbance of dissolved formazan crystal at 540 and 690 nm was measured using a 96-well plate reader (ELx800 Absorbance Microplate Reader).

$$[(\text{absorbance of cell control} - \text{absorbance of blank}) - (\text{absorbance of treatment} - \text{absorbance of blank})] / (\text{absorbance of cell control} - \text{absorbance of blank}) \times 100\%$$

DNA Content Analysis. HK-1 cells (3×10^5/well) were seeded onto 35 mm Petri dish for overnight. The cells were treated with **2** (100 nM) for 6 h in dark. The cells were then irradiated (1−4 J/cm^2) as described above. At 24 h post-PDT, both floating and adherent cells were collected, washed with PBS twice and then fixed in 70% ethanol for at least 1 h at 4 °C. After fixation, the cells were stained with DNA-binding buffer (40 μg/mL propidium iodide, 1 mg/mL RNase, 0.1% Triton X-100 in PBS) for 30 min. The fluorescence profiles of the stained cells were analyzed using the FACSCalibur Flow Cytometer (Becton−Dickinson).[23] Laser with a wavelength of 488 nm was used for excitation, and the fluorescence signal was detected using the FL-2 channel (λ_{em} = 564−606 nm). At least 10 000 events were counted. DNA content was analyzed using the Cell Quest and the Modfit LT Version 3.0 Software.

Staining of Apoptotic Nuclei. Hoechst 33258 was used in the staining of apoptotic nuclei.[24] Overnight cultured HK-1 cells were treated with **2** (100 nM) for 6 h in dark and then irradiated (1−4 J/cm^2) as described previously. At 3 and 16 h after PDT, detached and adherent cells were collected and fixed with 4% paraformaldehyde in PBS for 15 min. Cell membrane was permeabilized with absolute methanol for 20 min, followed by staining with Hoechst 33258 (0.12 μg/mL) in PBS for 15 min. Fluorescence images of apoptotic nuclei were visualized and captured under a fluorescence microscope (Zeiss, Axioskop2).

Two-Photon-Induced Confocal Microscopic Imaging of Rh-SiPc Conjugates. HeLa cells (1×10^5) were seeded onto coverslip in 35-mm culture dishes for overnight. The cells were initially incubated with Rh-SiPc-Rh (**2**, 5 μM), Rh-SiPc (**3**, 5 μM), or C_7-SiPc-C_7 (**4**, 5 μM) for 6 h in dark. The two-photon-induced fluorescent signals of **2**, **3**, and **4** were captured using the Leica SP5 (upright configuration) confocal microscope equipped with a femtosecond-pulsed Ti:Sapphire laser (Libra II, Coherent) inside the tissue culture chamber (5% CO_2, 37 °C). The excitation beam produced by the femtosecond laser, which was tunable from 680 to 1050 nm, was focused on the adherent cells through a 40× oil immersion objective.

dx.doi.org/10.1021/ic201178e | *Inorg. Chem.* 2012, 51, 812−821

The time-lapse images (0−30 min, one laser shot per min) were obtained with femtosecond laser excitation at 850 nm (laser power ~8 mW).

Two-Photon Absorption Measurement. Two-photon absorption spectra of **2**, **3**, and **4** were measured at 850 nm by the open-aperture *Z*-scan method[25] using 100-fs laser pulses with a peak power of 276 GW cm^{-2} from an optical parametric amplifier operating at a 1-kHz repetition rate generated from a Ti:Sapphire regenerative amplifier system. The laser beam was split into two parts by a beam splitter. One was monitored by a photodiode (D1) as the incident intensity reference, I_0, and the other beam was detected by the photodiode (D2) as the transmitted intensity. After passing through a lens with $f = 20$ cm, the laser beam was focused and passed through a quartz cell. The position of the sample cell, z, was moved along the laser-beam direction (z axis) by a computer-controlled translatable table so that the local power density within the sample cell could be changed under the constant incident intensity laser power level. Finally, the transmitted intensity from the sample cell was detected by the photodiode D2 interfaced to a computer for signal acquisition and averaging. Each transmitted intensity data represent an average of over 100 measurements. Assuming a Gaussian beam profile, the nonlinear absorption coefficient β can be obtained by curve fitting to the observed open-aperture traces, $T(z)$, with eq 1,

$$T(z) = 1 - \frac{\beta I_0 (1 - e^{-\alpha_0 l})}{2a_0[1 + (z/z_0)]^2} \quad (1)$$

where a_0 is the linear absorption coefficient, l is the sample length (1 mm quartz cell) and z_0 is the diffraction length of the incident beam.

After the nonlinear absorption coefficient β was obtained, the two-photon absorption cross-section σ_2 of the sample molecule (in units of GM, where 1 GM = 10^{-50} cm^4 s $photon^{-1}$) can be calculated using eq 2

$$\sigma_2 = \frac{1000\beta h\nu}{N_A d} \quad (2)$$

where N_A is the Avogadro constant, d is the concentration of the sample compound in solution, h is the Planck constant, and ν is the frequency of the incident laser beam.

Singlet Oxygen Quantum Yield Measurement. Singlet oxygen was detected directly by its phosphorescence emission at 1270 nm using an InGaAs detector on a PTI QM4 luminescence spectrometer. The singlet oxygen quantum yields (Φ_Δ) of the test compounds were determined in $CHCl_3$ by comparing the singlet oxygen emission intensity of the sample solution to that of a reference compound (H_2TPP, $\Phi_\Delta = 0.55$ in $CHCl_3$)[26] according to eq 3[27]

$$\Phi_\Delta^S = \Phi_\Delta^{REF} \times \left(\frac{n_S}{n_{REF}}\right)^2 \frac{G_\Delta^S}{G_\Delta^{REF}} \times \frac{A_{REF}}{A_S} \quad (3)$$

where Φ_Δ is the singlet oxygen quantum yield, G_Δ is the integrated emission intensity, A is the absorbance at the excitation wavelength, n is the refractive index of the solvent. Superscripts REF and S correspond to the reference and the sample, respectively. In all measurements, the $^1O_2$ emission spectra were obtained using an excitation with the absorbance set at 0.05 in order to minimize reabsorption of the emitted light.

Synthesis of Tetraethylene Glycol Rhodamine B, 1. A mixture of tetraethylene glycol monoiodide (912 mg, 3 mmol), rhodamine B (1.437 g, 3 mmol) and K_2CO_3 (415 mg, 3 mmol) in DMF (50 mL) was heated at 70 °C for three days. The product mixture was filtered and the filtrate was evaporated under vacuum. The solid obtained was dissolved in a minimum amount of CH_2Cl_2 and then loaded onto a silica gel column. The first purple-red band, which corresponded to the unreacted rhodamine B, was eluted with EtOAc/MeOH/Et_3N (85:10:5). The second purple-red band, which corresponded to product **1**, was eluted with CH_2Cl_2/MeOH (75/25). Removal of solvent by evaporation afforded the purple-brown color sticky product **1** (987 mg, 53.1%): UV/vis [CH_2Cl_2, λ_{max}/nm (log ε)] 521 (3.94), 557 (4.66); ^1H NMR (400 MHz, CD_2Cl_2): δ = 8.28 (d, J = 7.6 Hz, 1H; H_{ar}), 7.77 (m, 2H; H_{ar}), 7.24 (d, J = 7.6 Hz, 1H; H_{ar}), 7.02 (d, J = 9.6 Hz, 2H; H_{ar}), 6.78 (d, J = 9.6 Hz, 2H; H_{ar}), 6.72 (s, 2H; H_{ar}), 4.08 (t, J = 4.7 Hz, 2H; OCH_2), 3.52 (m, 8H; NCH_2CH_3), 3.45 (m, 14H; OCH_2), 2.56 (broad s, 1H; O*H*), 1.25 (t, J = 7.1 Hz, 12H; NCH_2CH_3) ppm; ^{13}C NMR (100 MHz, CD_2Cl_2) δ = 165.3, 159.5, 158.2, 155.9, 134.0, 133.4, 131.8, 131.7, 130.8, 130.5, 130.2, 114.5, 113.9, 96.5, 72.9, 70.9,70.8, 70.7, 70.6, 69.0, 65.1, 61.8, 46.5, 12.8 ppm; HRMS (MALDI) m/z calcd for $[C_{36}H_{47}N_2O_7]^+$ 619.3378 [M − Cl] $^+$; found 619.3374; Δ_m = −0.65 ppm.

Synthesis of Rh-SiPc-Rh (2) and Rh-SiPc (3). A mixture of tetraethylene glycol rhodamine B (**1**, 123.8 mg 0.2 mmol), $SiPcCl_2$ (61.2 mg, 0.1 mmol) and 0.5 mL dried pyridine in dried toluene (20 mL) was refluxed for 24 h. After cooling to room temperature, the solvent, which contained the unreacted **1** and the byproduct SiPc-tetraethylene glycol without the Rh B, was poured out. The sticky blue liquid mixture adhered to the bottom of the reaction flask was dissolved in a minimum volume of CH_2Cl_2 and loaded onto a basic Al_2O_3 column. Product **3** was eluted with CH_2Cl_2/MeOH (80:20) as a blue band and product **2** was eluted with CH_2Cl_2/MeOH (75:25) as a purple-blue band. Removal of solvent by passage of air stream afforded the purplish blue solid product **3** (7.76 mg, 4.2%) and the deep blue-pale purple colored solid product **2** (19.4 mg, 10.5%). Both products were purified by recrystallization from CH_2Cl_2/Et_2O. **2**: UV/vis [CH_2Cl_2, λ_{max}/nm (log ε)] 353 (4.63), 558 (4.89), 607 (4.13), 645 (4.09), 675 (4.93); ^1H NMR (400 MHz, CD_2Cl_2) δ = 9.54 (d, J = 2.7 Hz, 8H; *Pc*-1,4-H_{ar}), 8.29 (d, J = 2.7 Hz, 8H; *Pc*-2,3-H_{ar}), 8.04 (d, J = 7.6 Hz, 2H; Rh-H_{ar}), 7.63 (t, J = 7.6 Hz, 2H; Rh-H_{ar}), 7.49 (t, J = 7.8 Hz, 2H; Rh-H_{ar}), 7.20 (d, J = 7.8 Hz, 2H; Rh-H_{ar}), 6.86 (d, J = 9.4 Hz, 4H; Rh-H_{ar}), 6.62 (d, J = 9.4 Hz, 4H; Rh-H_{ar}), 6.54 (s, 4H; Rh-H_{ar}), 3.81 (t, J = 4.5 Hz, 4H; OCH_2), 3.45 (m, 16H; NCH_2CH_3), 3.06 (t, J = 4.5 Hz, 4H; OCH_2), 2.91 (t, J = 4.7 Hz, 4H; OCH_2), 2.75 (t, J = 4.7 Hz, 4H; OCH_2), 2.30 (t, J = 4.7 Hz, 4H; OCH_2), 1.58 (t, J = 4.7 Hz, 4H; OCH_2), 1.12 (m, 24H; NCH_2CH_3), 0.27 (t, J = 5.6 Hz, 4H; Si-OCH_2CH_2O), −2.05 ppm (t, J = 5.6 Hz, 4H; Si-OCH_2CH_2O); HRMS (MALDI) m/z calcd for $[C_{104}H_{108}N_{12}O_{12}Si]^{2+}$ 1777.7901 [M − 2Cl]$^+$; found 1777.7910; Δ_m = 0.46 ppm. **3**: UV/vis [CH_2Cl_2, λ_{max}/nm (log ε)] 343 (4.57), 559 (4.73), 611 (4.24), 649 (4.16), 679 (4.99); ^1H NMR (400 MHz, CD_2Cl_2) δ = 9.49 (m, 8H; *Pc*-1,4-H_{ar}), 8.23 (d, J = 7.6 Hz, 1H; Rh-H_{ar}), 8.18 (m, 8H; *Pc*-2,3-H_{ar}), 7.67 (m, 2H; Rh-H_{ar}), 7.30 (d, J = 7.6 Hz, 1H; Rh-H_{ar}), 6.92 (d, J = 9.4 Hz, 2H; Rh-H_{ar}), 6.52 (d, J = 9.4 Hz, 2H; Rh-H_{ar}), 6.34 (s, 2H; Rh-H_{ar}), 4.01 (t, J = 4.6 Hz, 2H; OCH_2), 3.20 (m, 10H; OCH_2 + NCH_2CH_3), 2.95 (t, J = 4.6 Hz, 2H; OCH_2), 2.69 (t, J = 4.6 Hz, 2H; OCH_2), 2.25 (t, J = 4.8 Hz, 2H; OCH_2), 1.56 (t, J = 4.8 Hz, 2H; OCH_2), 1.00 (t, J = 7.2 Hz, 12H; NCH_2CH_3), 0.29 (t, J = 5.4 Hz, 2H; $SiOCH_2CH_2O$), −2.00 (t, J = 5.40 Hz, 2H; $SiOCH_2CH_2O$) ppm; HRMS (MALDI) m/z calcd for $[C_{68}H_{62}N_{10}O_8Si]^+$ 1175.4594 [M − Cl]$^+$; found 1175.4604; Δ_m = 0.85 ppm.

Synthesis of C_7-SiPc-C_7 (4). A mixture of tri(ethyl glycol)-monomethylether (79 μL, 0.5 mmol), $SiPcCl_2$ (30.5 mg, 0.05 mmol), and anhydrous K_2CO_3 (27.6 mg, 0.2 mmol) in dried toluene (10 mL) was refluxed for 14 h. After it was cooled to room temperature, the mixture was directly loaded onto a basic Al_2O_3 column. Product **4** was eluted with CH_2Cl_2/MeOH (80:5) as a green band. Removal of solvent by evaporation afforded a green solid product **4** (6.7 mg, 15.6%). The crude product was purified by recrystallization from CH_2Cl_2/Et_2O: UV/vis [CH_2Cl_2, λ_{max}/nm (log ε)] 354 (4.01), 605 (3.80), 643 (3.72), 673 (4.62); ^1H NMR (400 MHz, CD_2Cl_2) δ = 9.63 (m, 8H; *Pc*-1,4-H_{ar}), 8.34 (m, 8H; *Pc*-2,3-H_{ar}), 3.14 (s, 6H; OCH_3), 3.12 (t, J = 4.6 Hz, 4H; OCH_2), 2.95 (t, J = 4.8 Hz, 4H; OCH_2), 2.45 (t, J = 4.9 Hz, 4H; OCH_2), 1.67 (t, J = 4.9 Hz, 4H; OCH_2), 0.38 (t, J = 5.7 Hz, 4H; $SiOCH_2CH_2O$), −1.92 (t, J = 5.7 Hz, 4H; $SiOCH_2CH_2O$) ppm; ^{13}C NMR (100 MHz, CD_2Cl_2) δ = 29.70, 54.68, 58.79, 68.56, 69.30, 69.70, 71.46, 123.64, 130.83, 135.98, 149.21 ppm; HRMS (MALDI) m/z calcd for $[C_{46}H_{46}N_8O_8SiNa]^+$ 889.3100 [M + Na]$^+$; found 889.3149; Δ_m = 5.51 ppm.

X-ray Crystallography. X-ray diffraction data were collected at 173 K using graphite-monochromated Mo Kα radiation (λ = 0.71073 Å) on a Bruker Axs SMART 1000 CCD diffractometer. The collected frames were processed with the software SAINT+[28] and an absorption

dx.doi.org/10.1021/ic201178e | *Inorg. Chem.* 2012, 51, 812−821

Scheme 1. Synthesis Route to the Si(IV)Pc-Rhodamine B Conjugates, 2 and 3, and the Si(IV)Pc with Axially Ligated Polyethylene Glycol, 4

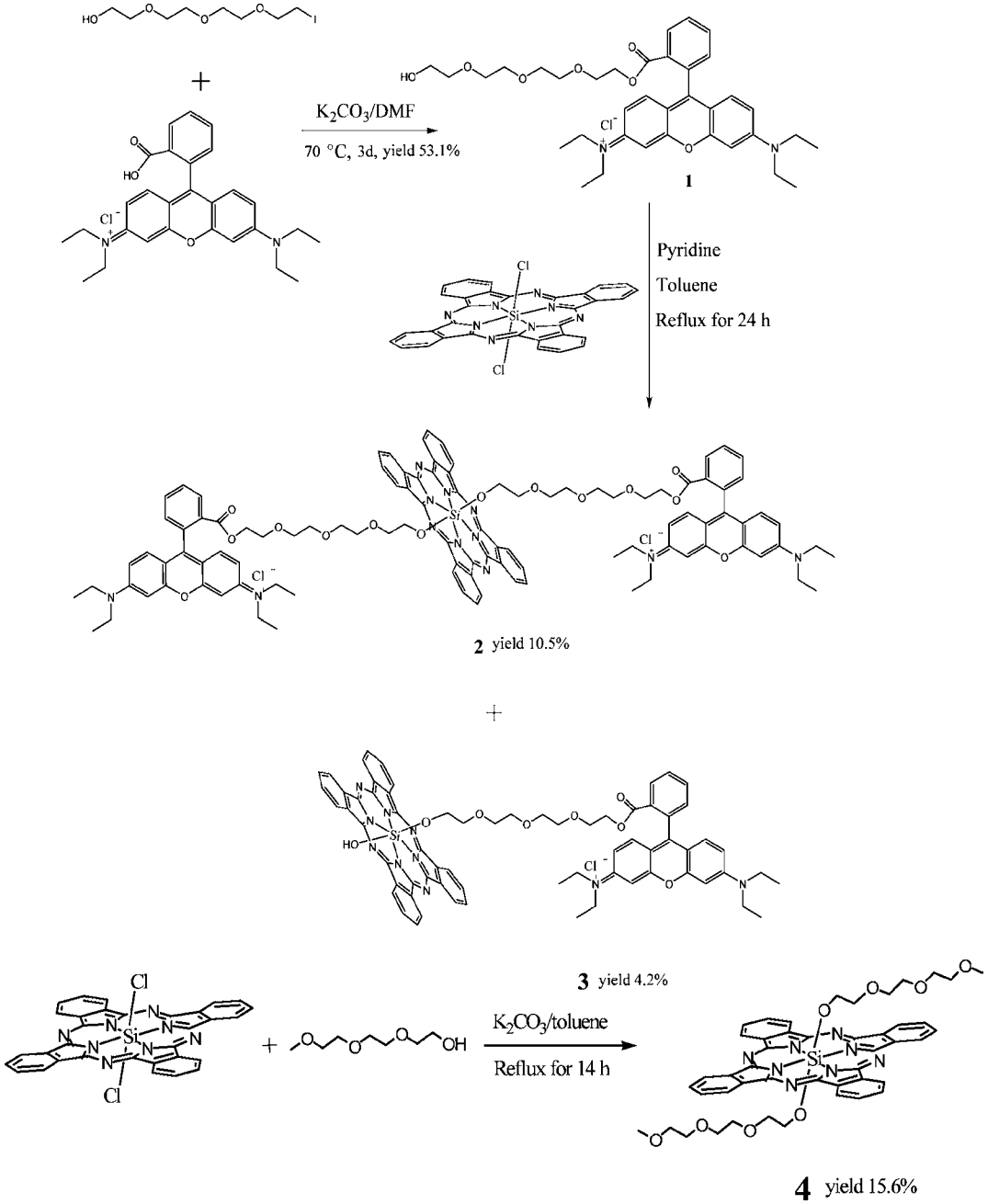

correction (SADABS)[29] was applied to the collected reflections. The structure was solved by the Direct method (SHELXTL)[30] in conjunction with standard difference Fourier techniques and subsequently refined by full-matrix least-squares analyses on F^2. Hydrogen atoms were generated in their idealized positions and all non-hydrogen atoms were refined anisotropically. Crystal data for **1**: $C_{46}H_{46}N_8O_8Si$; M = 867.00; triclinic; space group $\bar{P}1$; a = 7.9377(8), b = 10.210(1), c = 13.216(1) Å; α = 94.452(2), β = 94.984(2), γ = 105.604(2)°; V = 1022.1(2) Å^3; T = 173(2) K; Z = 1; reflections collected/unique, 6493/4666, R_{int} = 0.0184; final R indices [$I > 2\sigma(I)$], R_1 = 0.0366, R_2 = 0.0969 for 4162 observed reflections; R indices (all data), R_1 = 0.0415, R_2 = 0.1013; GOF = 1.040; CCDC 779323.

RESULTS AND DISCUSSION

Synthesis of Silicon(IV) Phthalocyanine-Rhodamine B Conjugates. The synthetic route for the two silicon(IV) phthalocyanine-rhodamine B conjugates, **2** and **3**, is shown in Scheme 1. Briefly, tetraethylene glycol monoiodide was prepared according to the literature procedure.[31] Treatment of the commercially available Rh B with tetraethylene glycol monoiodide in the presence of K_2CO_3 in DMF gave the tetraethylene glycol-rhodamine B, **1**, in 53% yield after its separation from the unreacted Rh B by silica gel column chromatography. Further washing of the silica gel column with the eluting solvent allowed a second harvest of **1**, resulting in a combined yield of 70%.

Products **2** and **3** were synthesized according to the literature procedure.[32] Bases, such as K_2CO_3, NaH, quinoline, DMF, pyridine, have been used to render silicon(IV) phthalocyanine dichloride ($SiPcCl_2$) reactive to hydroxyl derivatives. In our preparation of **2** and **3**, K_2CO_3 and pyridine were tried. Both bases gave a number of byproduct of SiPc containing one and

dx.doi.org/10.1021/ic201178e | Inorg. Chem. 2012, 51, 812−821

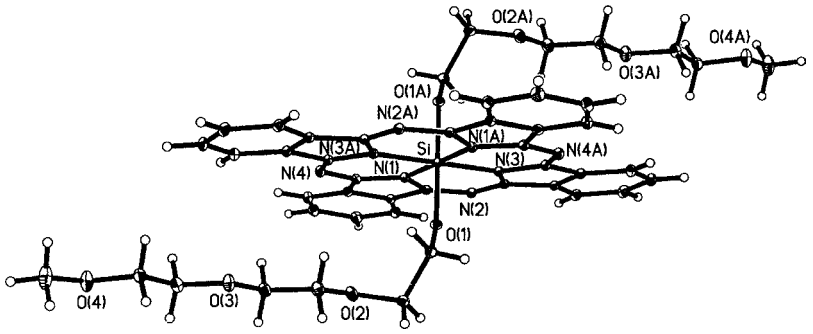

Figure 1. Perspective drawing of **4**, with the thermal ellipsoids drawn at the 25% probability level. Selected bond lengths (Å) and angles (deg): Si–N(1) 1.920(1), Si–N(3) 1.9333(9), Si–O(1) 1.6971(8); N(1)–Si–N(3) 89.88(4), N(1)–Si–O(1) 86.61(4).

two polyethers without the Rh B. These byproduct were identified after TLC separation by MALDI-TOF-MS and NMR. The yields of **2** and **3** were found to be similar for both bases. However, with pyridine as base, products **2** and **3** were found in the sticky liquid adhered to the bottom of the reaction flask, while the byproduct and the starting material, **1**, were present in the toluene solvent bulk and were therefore removed readily. Products **2** and **3** were then isolated and purified by basic alumina column chromatography. Dichloromethane/methanol was used as the eluting solvent to elute products **2** (yield 10.5%) and **3** (yield 4.2%) from the basic alumina column. Since methanol has been reported to replace the axial ligand of SiPc,[32,33] other mixed solvents without methanol, such as CH_2Cl_2/acetonitrile, CH_2Cl_2/tetrahydrofuran (THF), and ethyl acetate/THF, were tried as eluent but to no avail. This observation suggests that the cations present in **2** and **3** might have increased their adsorption to the basic alumina column, thus reducing the recoverable yields. Another reason for the low observed yield could be the result of the displacement of the axially ligated Rh B by the methanol used in elution. In contrast, product **4** is more stable and no obvious decomposition was observed during purification. Both **2** and **3** are soluble in most organic solvents, such as CH_2Cl_2, $CHCl_3$, methanol, acetonitrile, THF, dimethylformamide, and dimethylsulfoxide, and they even showed slight solubility in water, giving purple red solutions.

All products were characterized by NMR and high-resolution mass spectrometry. Compared to the ^{1}H NMR spectrum of Rh B, product **1** showed two additional peaks at δ 3.56 (14 H) and 4.08 ppm (2H), corresponding to the ethylene protons of the tetra(ethylene glycol) that are distal and proximal, respectively, to the Rh B (Supporting Information Figure S1). The eight new carbon peaks found at δ 62–73 ppm in the ^{13}C NMR spectrum of **1** are due to the eight carbon atoms of the tetra(ethylene glycol). MALDI-TOF mass spectrum of **1** gave a peak at m/z of 619.3374, which compared favorably (Δ_m = −0.65 ppm) to the calculated m/z of 619.3378 for the $[M - Cl]^+$ ion of **1** (Supporting Information Figure S2)

The ^{1}H NMR spectra of **2**, **3**, and **4** showed two downfield groups of peaks (δ = 8–10 ppm) typical of the α- and β-protons of the *Pc* ring (Supporting Information Figures S3, S5, and S7). Because of the strong ring current effect of the *Pc*, the signals of the ethylene glycol protons of **2**, **3**, and **4** are upfield shifted when compared to **1**. These ethylene glycol signals appeared as eight four-proton triplets from δ −2.05 to 3.81 ppm for **2**; seven two-proton triplets from δ −2.00 to 4.01 ppm and another two-proton signal overlapped with Rh B methylene group at δ 3.20 ppm for **3**; and six four-proton triplets from δ −1.91 to 3.12 for **4**. The methoxy protons of **4** appeared as a sharp singlet at δ 3.14 ppm. High resolution mass spectra were also measured to confirm the identity of these compounds. Molecular ion peak at m/z 1777.7910 observed for **2** is in good agreement with the calculated m/z value of 1777.7901 for the $[M-2Cl]^+$ ion of **2** (Supporting Information Figure S4). For **3**, two major molecular ion peaks were seen at m/z 1175.4604 and m/z 1158.4113, corresponding to its $[M - Cl]^+$ and $[M - Cl - OH]^+$ ions, respectively (Supporting Information Figure S6). Three major molecular ion peaks were observed for **4**, that is, at m/z 889.3149, m/z 728.3082 and m/z 703.2029, which corresponded to its $[M+Na]^+$ ion, [M–tri(ethyl glycol)-monomethylether+Na]$^+$ ion and [M–tri(ethyl glycol)-monomethyl ether]$^+$ ion, respectively (Supporting Information Figure S8). The molecular structure of **4** was also confirmed by X-ray crystallography (see Figure 1). The asymmetric unit consists of half of a molecule and the two halves are related by a center of inversion at the Si atom. The Si center is six-coordinate with four *Pc* nitrogen donor atoms and two axial oxygen donors from the polyethylene glycol units arranged in an octahedral environment.

Photophysical Properties of 2 and 3. The UV/vis spectra of **2** and **3**, together with those of **1** (Rh) and **4** (C_7-SiPc-C_7) in CH_2Cl_2 are shown in Figure 2. The simultaneous appearance of the rhodamine and SiPc characteristic absorptions

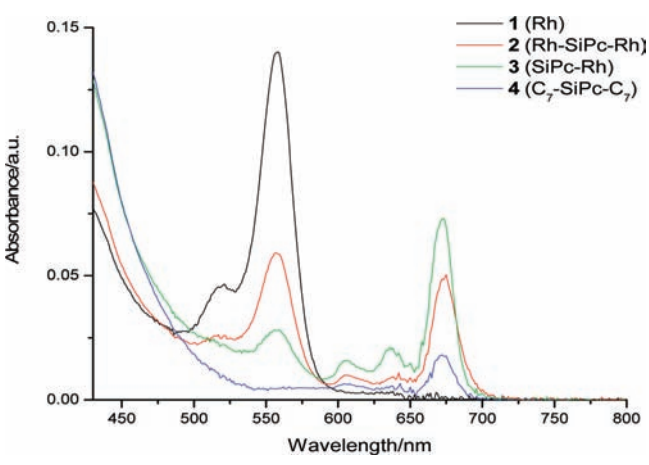

Figure 2. UV/vis spectra of the **1** (Rh, ε_{520nm} = 46600; ε_{557nm} = 145000), **2** (Rh-SiPc-Rh, ε_{520nm} = 26400; ε_{557nm} = 5990; ε_{607nm} = 46600; ε_{673nm} = 50000), **3** (SiPc-Rh (ε_{558nm} = 28700; ε_{607nm} = 16490; ε_{639nm} = 21000; ε_{672nm} = 74000), and **4** (C_7-SiPc-C_7, ε_{672nm} = 16400) at concentration of ~1 μM.

dx.doi.org/10.1021/ic201178e | *Inorg. Chem.* 2012, 51, 812–821

in the spectra of **2** and **3** confirms their rhodamine-SiPc conjugate structure. Furthermore, the absorption intensity of **2** at 557 nm (rhodamine absorption peak) is ~2-fold to that of **3**. This observation is consistent with the ligation of two and one Rh B moiety in **2** and **3**, respectively. Figure 3 shows the absorption and emission spectra of **2** as a function of its concentration in CH_2Cl_2. The spectra exhibit typical features of nonaggregated phthalocyanines. The inset in Figure 3a shows a plot of the absorption intensities of the SiPc Q-band and rhodamine versus the concentration of **2**. The inset in Figure 3b shows a plot of the emissions of **2** due to its Rh B (560 nm) and SiPc (681 nm) moieties versus its concentration. These linear plots observed in both the absorption and emission spectra of **2** shows that this compound is essentially free from aggregation in the indicated concentration ranges in CH_2Cl_2.

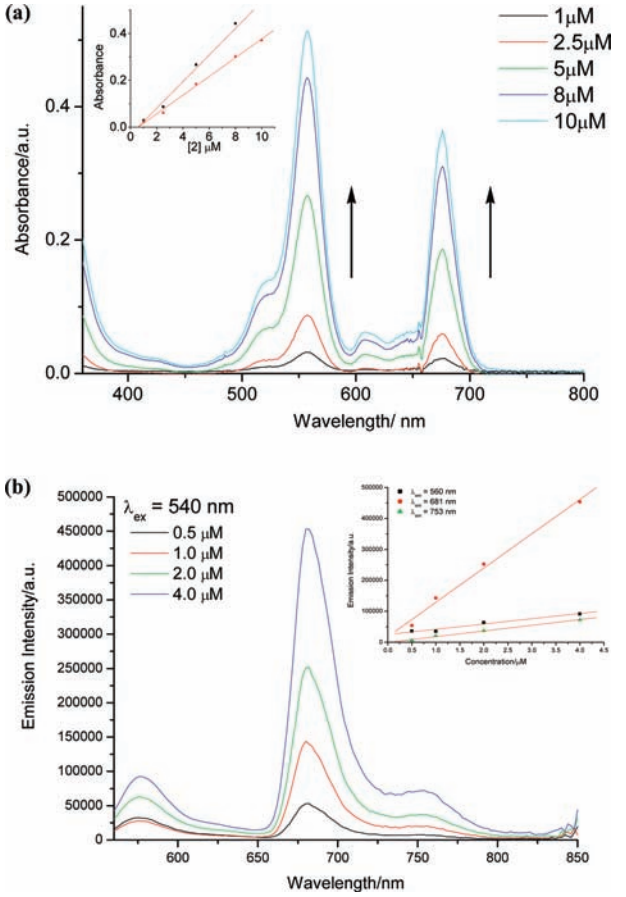

Figure 3. (a) UV/vis spectra of different concentrations of **2** in CH_2Cl_2. The inset shows a plot of the absorbance of **2** at 557 nm (square), due to the Rh B moiety, and at 672 nm (triangle), due to the SiPc moiety, as a function of its concentration. (b) Emission spectra of different concentrations of **2** in CH_2Cl_2. The inset shows a plot of the emission of **2** at 560 nm (square), due to the Rh B moiety, at 681 nm (circle) and at 753 nm (triangle), due to the SiPc moiety, as a function of its concentration.

The fluorescence spectra of **2** and **3** are shown in Figure 4. For both conjugates, excitation of the rhodamine band at 515 nm led to emissions from both the Rh and the *Pc* moieties while excitation of the *Pc* chromophore at 640 nm resulted in emission exclusively from the *Pc* moiety. Furthermore, the emission from the *Pc* moiety excited at 515 nm coincided with the emission obtained from excitation at 640 nm. These observations indicate an intramolecular energy transfer from the excited Rh B to the *Pc* moiety in **2** (λ_{em} = 681 nm) and **3** (λ_{em} = 688 nm), very similar to that observed previously for Zn(II)Pc with peripherally substituted rhodamines.[19] These results clearly indicate that such intramolecular energy transfer from Rh to *Pc* can occur readily with either axially ligated or peripherally substituted rhodamines.

Recently, phthalocyanines (H_2Pc and ZnPc) peripherally substituted by four tetraphenylporphyrins (H_2TPP and ZnTPP) via alkyne linkages in a windmill fashion was synthesized and the intramolecular porphyrin-to-Pc energy transfer studied.[36] Compared to the almost quantitative TPP-to-Pc energy transfer, the efficiency of Rh-to-Pc energy transfer in **2** and **3** is significantly lower. The difference is presumably due to the long and nonconjugative alkoxy linkage between the donor and acceptor in **2** and **3** as compared to the short and conjugative alkyne linkage between TPP and Pc.

Production of Singlet Oxygen from 2 and 3. To assess their potential as effective PDT agents, the $^1O_2$ production capabilities of these Rh-SiPc conjugates were measured based on the phosphorescence intensities of the $^1O_2$ produced upon photoirradiation of these compounds. Figure 5a shows the $^1O_2$ phosphorescence spectra of **2**, **3**, and H_2TPP in $CHCl_3$. Using the $^1O_2$ quantum yield of H_2TPP (Φ_Δ = 0.55 ± 0.11) as the reference standard,[21,26] the relative Φ_Δ of Rh-SiPc-Rh (**2**) and Rh-SiPc (**3**) were estimated to be 0.48 ± 0.11 and 0.25 ± 0.11,

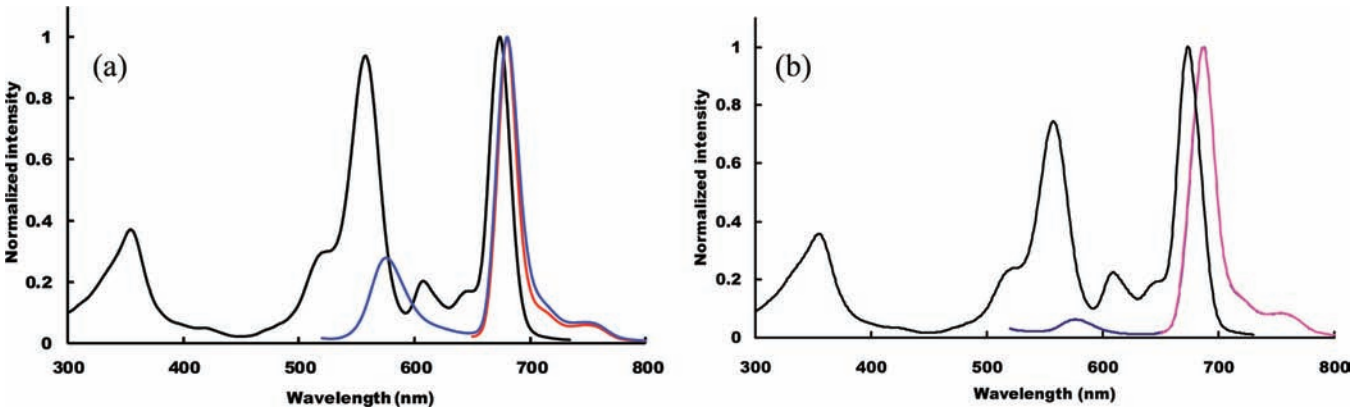

Figure 4. Normalized excitation spectrum (black, monitored at 750 nm) and fluorescence spectra (blue, λ_{exc} = 515 nm and red, λ_{exc} = 640 nm) of **2** (a) and **3** (b) in CH_2Cl_2 (~1.0×10^{-6} M). Note that the emissions from the *Pc* moiety of **2** and **3** excited at 515 and 640 nm coincide almost completely.

dx.doi.org/10.1021/ic201178e | *Inorg. Chem.* 2012, 51, 812–821

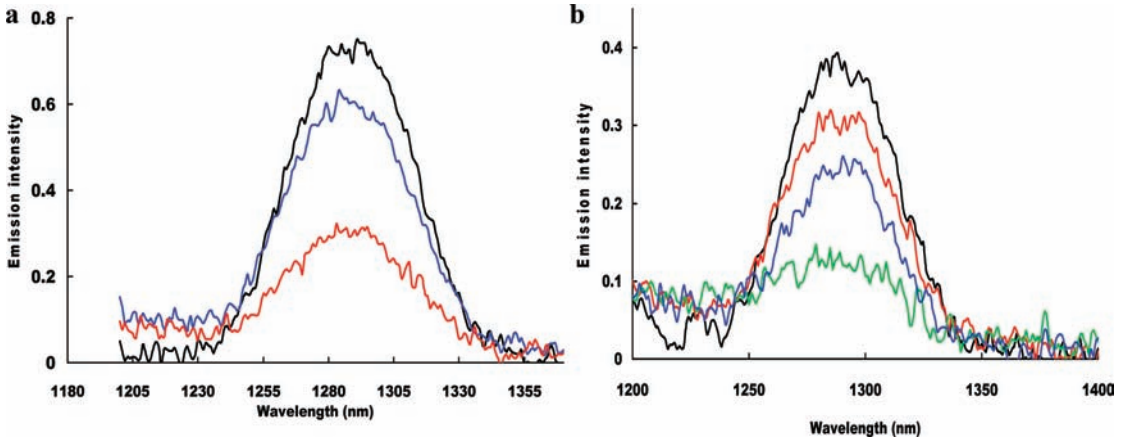

Figure 5. Near-IR phosphorescence spectra of the $^1O_2$ generated from the following photosensitizers: (a) H_2TPP (black), Rh-SiPc-Rh (**2**, blue), and Rh-SiPc (**3**, red) excited at 549 nm in $CHCl_3$; (b) ZnPc (black), Rh-SiPc-Rh (**2**, red), C_7-SiPc-C_7 (**4**, blue), and Rh-SiPc (**3**, green) excited at 666 nm in toluene. Note that the concentrations of the photosensitizers used are different between a and b.

respectively, when excited at the Rh B absorption maximum of 549 nm. Since rhodamine has very low $^1O_2$ production capability,[37] the substantial $^1O_2$ generation observed must be the result of an energy transfer from the photoexcited Rh B to the *Pc* moiety which produced the $^1O_2$ observed in **2** and **3**.

To evaluate the $^1O_2$ production capability of the SiPc moiety alone, the $^1O_2$ phosphorescence spectrum of C_7-SiPc-C_7 (**4**), soluble in toluene, upon photoexcitation at 549 nm was measured and is shown in Figure 5b, together with those spectra obtained from ZnPc, **2** and **3**, measured under identical conditions. The relative Φ_Δ estimated for ZnPc, Rh-SiPc-Rh (**2**), Rh-SiPc (**3**), and C_7-SiPc-C_7 (**4**) in toluene were 0.58 ± 0.11, 0.50 ± 0.10, 0.23 ± 0.07, and 0.38 ± 0.08, respectively. These measurements show that (1) SiPc is quite capable of producing singlet oxygen even when excited at a nonoptimal wavelength (e.g., **4** with Φ_Δ = 0.38 at 549 nm), (2) the ligation of two Rh B to SiPc increased its $^1O_2$ quantum yield (**2** with Φ_Δ = 0.50), and (3) the presence of an additional Rh B chromophore in **2** resulted in a 2-fold increase in the $^1O_2$ quantum yield of **3** (Φ_Δ = 0.23). Thus, while the introduction of the Rh moiety to SiPc is mainly for its mitochondria-targeting function in cells (vide infra), its presence also allows for $^1O_2$ generation from Pc's at shorter wavelengths that support the Rh-to-Pc energy transfer.

Two-Photon Absorption Properties of 2, 3, and 4. Recent studies showed that $^1O_2$ can also be generated via two-photon excitation of a sensitizer.[38] In this approach, a chromophore such as Rh B which absorbs at λ < 650 nm, that is, in the tissue nontransparent spectral region, by one-photon absorption, can be excited by two-photon absorption (2PA) at λ > 650 nm, which allows much better depth penetration through tissues. Other advantages of 2PA-PDT include (1) high-resolution (femtoliter scale) targeting with pinpoint accuracy, thus minimizing photodamage to tissues along the beam path of a one-photon PDT, (2) negligible photobleaching of the sensitizing chromophore, and (3) minimal endogenous autofluorescence.[39,40]

To assess the potential of **2** and **3** as 2PA-PDT agents, we measured their two-photon absorption cross sections, σ_2, by the open aperture *Z*-scan method.[24] The results are shown in Figure 6, from which the 2PA cross sections of **2** and **3** were derived to be 1494 GM and 706 GM (where GM = 10^{-50} cm^4 s photon^{-1}), respectively, at 850 nm. Compared to the σ_2 of Rh B, that is, ~120 GM at 850 nm,[42] an apparent 6-fold enhancement in σ_2 for each Rh B chromophore can be seen in these Rh-SiPc conjugates. To ascertain that this enhancement of σ_2 in **2** and **3** is derived principally from Rh B being ligated to SiPc and not from the SiPc moiety itself, we compared these σ_2 values to that of C_7-SiPc-C_7, **4**, which was measured to be 318 GM (data shown in Supporting Information Figure S11). This comparison clearly shows that the enhancement of σ_2 in **2** and **3** is due to the ligation of Rh B to SiPc. This notion is corroborated by the 2-fold higher σ_2 value in **2**, with two ligated Rh B, as compared to that in **1**, with only one ligated Rh B. Such enhancement in two-photon absorption efficiency in **2** and **3** might be due to a possible intramolecular electron transfer

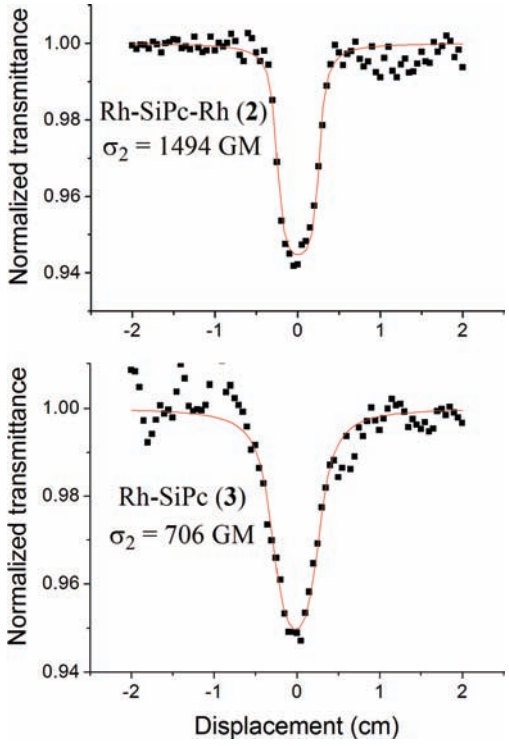

Figure 6. Open-aperture *Z*-scan traces of 0.1 mM of Rh-SiPc-Rh, (**2**, top panel) and Rh-SiPc, (**3**, bottom panel) excited at 850 nm. The 2PA cross sections determined for **2** and **3** were 1494 GM and 706 GM, respectively.

dx.doi.org/10.1021/ic201178e | *Inorg. Chem.* 2012, 51, 812–821

between Rh B and SiPc, particularly considering the short polyethylene glycol linkage between them. A more detailed photophysical study using transient absorption spectroscopy should shed more light on this issue. Nonetheless, the substantial σ_2 measured for **2** and **3** suggests that these conjugates possess potent 2PA-PDT activity.[42]

Subcellular Localization of 2 and 3. To ascertain the mitochondria-localizing ability of Rh-SiPc-Rh (**2**) and Rh-SiPc (**3**), the human nasopharyngeal carcinoma cells (HK-1) were costained with mitochondria-specific probe. Judging from the overlapping of the fluorescence signals (yellow dots) emitted by these Rh-SiPc conjugates (**2** and **3**, red dots) and the mitochondria-specific probe (Mito Tracker Green, green dots), both **2** (Supporting Information Figure S11c, upper panel) and **3** (Supporting Information Figure S11d, upper panel) were found to localize in the mitochondria of HK-1 cells. The localization of **2** and **3** in mitochondria was further confirmed by analyzing the fluorescence-intensity profile drawn across the cells. The fluorescence profiles of these Rh-SiPc conjugates along the arrow (Supporting Information Figures S11c and S11d, lower panels) are similar to the fluorescence profile of the mitochondria-specific probe. Furthermore, the patterns of colocalization of **2**, **3**, and Rh B (Supporting Information Figure S11a, upper panel) with the mitochondria-specific probe are very similar. In contrast, mitochondrial localization of C_7-SiPc-C_7 (Supporting Information Figure S11b, upper panel), which possesses no Rh moiety, was not observed. These observations indicate that Rh B functioned as a carrier for phthalocyanine to gain entry into the mitochondria. The mitochondria-localizing capability of **2** and **3** was also demonstrated in a noncancerous cell line, namely, human umbilical vein endothelial cells (HUVEC), which is shown in Supporting Information Figure S12.

The localizing properties of **2** and **4** in other subcellular organelles, namely, lysosomes, Golgi bodies and endoplasmic reticulum (ER), were also studied using the corresponding organelle-specific probes. The confocal microscopic images obtained from these colocalization experiments are shown in Supporting Information Figures S13, S14, and S15. No significant localization of **2** in lysosomes, Golgi bodies and endoplasmic reticulum in the HK-1 cells was seen (Supporting Information Figure S13). As for the C_7-SiPc-C_7 control (**4**), no significant organelle-specific localization in lysosomes, Golgi bodies and endoplasmic reticulum was detected (Supporting Information Figures S14 and S15). These observations, taken together, indicate an almost exclusive subcellular localization of the Rh-SiPc conjugate, **2**, in the mitochondria of these cells.

Photocytotoxicity of 2, 3 and 4 Toward HK-1 cells. The dark and photo-cytototoxicity of **2** and **3** were measured, together with Rh B and C_7-SiPc-C_7 (**4**), which served as the reference. The results are shown in Figure 7. With light doses from 1 to 4 J/cm^2, **2**, **3**, and **4** exhibited a dose-dependent cytotoxicity to the HK-1 cells. However, photocytotoxicity was not observed in the Rh B-treated HK-1 cells. In addition, no significant cytotoxicity (i.e., <10%) due to **2** and **3** was observed when the HK-1 cells were incubated with these Rh-SiPc conjugates without photoirradiation. Furthermore, the observed photocytotoxicity of **2**, **3**, and **4** does not correlate with the measured $^1O_2$ quantum yields (**2** > **4** > **3**) of these compounds, suggesting that their subcellular localization might exert a crucial influence on their photocytotoxicity. However, recently Saha et al showed that the amount of complexes taken up by the cells is also a key factor in determining their in vitro toxicities

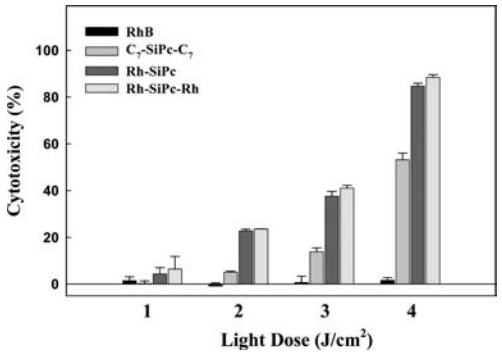

Figure 7. Photocytotoxicity of Rh B and Rh-SiPc conjugates in HK-1 cells. HK-1 cells (2×10^4 cells/well) were incubated in wells of 96-well plate for overnight. The cells were then treated with 100 nM of Rh B, C_7-SiPc-C_7 (**4**), Rh-SiPc (**3**), or Rh-SiPc-Rh (**2**) for 6 h in dark, followed by photoirradiation (1−4 J/cm^2) and MTT cytotoxicity assay. Results were expressed as the mean ± SD of three independent experiments.

(dark and light).[43] Further studies on the cellular uptake of these conjugates will be conducted to address this issue.

With the establishment of mitochondria-localizing and photocytotoxic properties of these Rh-SiPc conjugates, the next logical question is the mode of cell death (i.e., apoptosis vs. necrosis) induced by these conjugates. To determine the purported apoptotic cell death associated with the mitochondria-localizing property of Rh-SiPc conjugates, both nuclei staining method and flow cytometric DNA content analysis were performed on the HK-1 cells after PDT with **2**. No apoptotic nuclei formation was observed under the light dose 1 J/cm^2. However, apoptotic nuclei were observed for 3 h after PDT with light doses of 2 and 4 J/cm^2 (Supporting Information Figure S16).

The extent of apoptosis was further evaluated using flow cytometry and the results are shown in Supporting Information Figure S17. **2**-PDT increased the percentage of sub-G1 cells from 2% (control) to 10.9% (2 J/cm^2) to 20% (4 J/cm^2), indicating that **2**-PDT dose-dependently induced tumor cell apoptosis. Under the light dose of 1 J/cm^2, **2**-PDT was found to increase the percentage of G1 cells from 50.8% in the cell control group to 81.8% after PDT. This observation suggests that a low dose of **2**-PDT would induce G1 cell cycle arrest.

Two-Photon-Induced Cytotoxicity of 2, 3, and 4 Toward Human Cervical Carcinoma (HeLa) and Human Nasopharyngeal Carcinoma (HK-1) Cells. HK-1 cells were incubated with 0.5 μM of Rh-SiPc-Rh (**2**), Rh-SiPc (**3**), or C_7-SiPc-C_7 (**4**) containing no Rh B moiety, for 6 h. The cells were then excited at 850 nm, where Rh B and its SiPc conjugates, **2** and **3**, showed a two-photon absorption cross-section of ~120 GM,[42] 1494 GM and 706 GM, respectively. The confocal images were captured at one laser shot per minute for a total of 30 min. Figure 8 shows the confocal images of the cells at two-photon laser irradiation time t = 0, 5, 25, and 30 min. Bright fluorescent images (i.e., images captured at t = 0 min) were seen in cells treated with Rh-SiPc-Rh (**2**). The fluorescent intensity of the treated cells was time-dependently decreased. Similar changes in fluorescent intensity were also seen in cells treated with Rh-SiPc (**3**). There are two possible explanations for the reduced fluorescent intensity in cells after two-photon irradiation, namely, the photobleaching and the leakage of the Rh-SiPc conjugates from the damaged cell membrane after PDT. Photobleaching of the Rh-SiPc

dx.doi.org/10.1021/ic201178e | Inorg. Chem. 2012, 51, 812−821

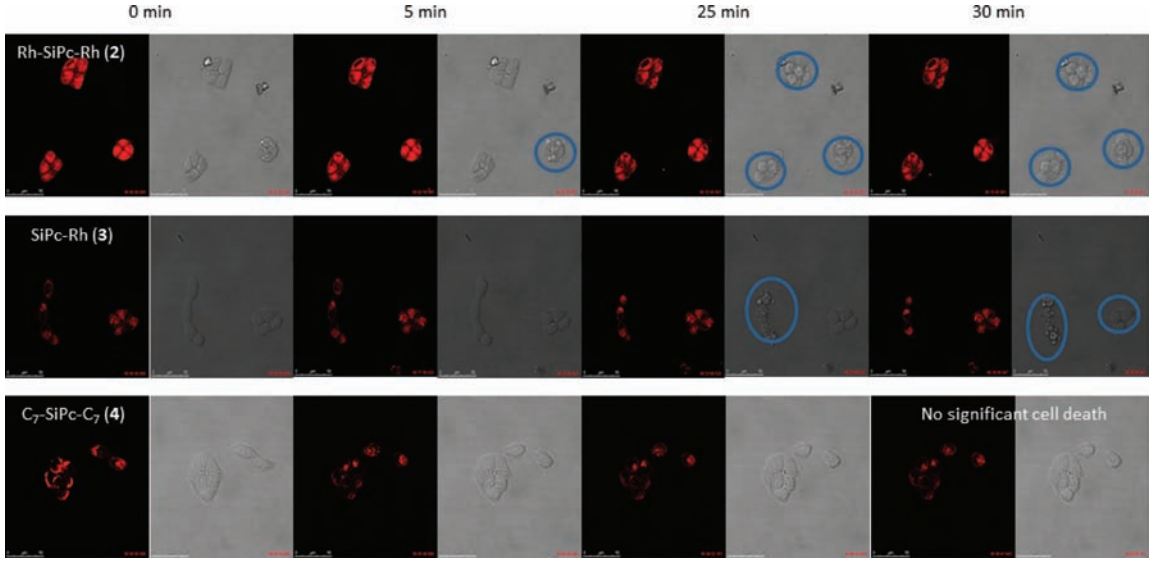

Figure 8. Confocal microscopic images of HK-1 cells treated with 0.5 μM of Rh-SiPc-Rh, (**2**, top), Rh-SiPc (**3**, middle), and C_7-SiPc-C_7 (**4**, bottom) obtained at various time points (0, 5, 25, and 30 min) under continuous laser flash excitation at 850 nm (one laser shot per min). The cells were incubated with **2**, **3**, and **4** for 6 h before the laser flash excitation.

conjugates is unlikely an explanation as photobleaching of chromophores resulting from two-photon excitation is considered negligible.[39−41] Leakage of the Rh-SiPc conjugates through the damaged membrane might be the possible explanation for the reduced fluorescent intensity of the stained cell. This explanation is supported by the fact that **2**- or **3**-PDT treated cells tend to round up, an early sign of cell death, after 2PA-PDT treatment. In contrast to Rh-SiPc and Rh-SiPc-Rh, the morphology of the **4**-PDT treated HeLa cells is similar to the cell image captured at before laser irradiation (i.e., t = 0 min). These observations clearly showed that **2** and **3** possess 2PA-PDT activities when excited at 850 nm whereas **4**, which bear no Rh B chromophore, displayed no significant 2PA-PDT activity. This experiment, however, precludes a quantitative comparison of the PDT activities of **2** and **3** resulted from one- versus two-photon excitation because the experimental conditions used (e.g., concentrations of the conjugates, cell type, etc.) were quite different. Nonetheless, the result does demonstrate substantial PDT activities of **2** and **3** induced via two-photon excitation of the Rh B chromophore potentially. In addition, Figure 8 also shows that **2** gave a stronger in vitro emission than **3** under two-photon excitation at 850 nm. This observation is consistent with the 2-fold higher σ_2 value measured for **2** than **3** (Figure 6).

CONCLUDING REMARKS

Two axially ligated rhodamine-Si(IV)-phthalocyanine conjugates, bearing one and two rhodamine B, were synthesized and their subcellular localizing and photocytotoxic properties induced by one- and two-photon excitation studied. These Rh-SiPc conjugates, **2**, exhibited an almost exclusive mitochondrial localizing property, together with strong photocytotoxic but low dark cytotoxic properties. Evidence of apoptotic cell death, which is consistent with their mitochondrial localization property, was also seen in the photocytotoxicity induced by these conjugates. These properties qualify them as highly promising PDT agents.

ASSOCIATED CONTENT

Supporting Information

NMR spectra, high-resolution MALDI-TOF mass spectra, in vitro imaging, and cytotoxicity results of the compounds synthesized. This material is available free of charge via the Internet at http://pubs.acs.org.

AUTHOR INFORMATION

Corresponding Author

*E-mail: dkwong@hkbu.edu.hk (D.W.J.); wkwong@hkbu.edu.hk (W.-K.W); nkmak@hkbu.edu.hk (N.-K.M.).

Author Contributions

Zhao, Chan, and Li made equal contribution as cofirst author

ACKNOWLEDGMENTS

The work described in this paper was partially supported by a grant from the Research Grants Council of the Hong Kong SAR, P.R. China (HKBU 202509 and HKBU 202210) and a grant from the Hong Kong Baptist University (FRG2/09-10/58). W.-Y. Wong and W.-K. Wong also thanks a grant from Areas of Excellence Scheme, University Grants Committee of HKSAR, China (Project No. [AoE/P-03/08]).

REFERENCES

(1) (a) Hasan, T.; Ortel, B.; Moor, A. C. E.; Pogue, B. W. In *Holland-Frei Cancer Medicine 6*; Kufe, D. W., Pollock, R. E., Weichselbaum, R. R., Bast, R. C., Jr., Gansler, T. S., Holland, J. F., Frei, E., III, Eds.; Decker, Hamilton, 2003, pp 605−622. (b) Triesscheijn, M.; Bass, P.; Schellens, J. H. M.; Stewart, F. A. *Oncologist* **2006**, *11*, 1034−1044. (c) Brown, S. B.; Brown, E. A.; Walker, I. *Lancet Oncol.* **2004**, *5*, 497−508. (d) Dolmans, D. E. J. G. J.; Fukumura, D.; Jain, R. K. *Nature Rev. Cancer* **2003**, *3*, 380−387.

(2) (a) Dougherty, T. J.; Gomer, C. J.; Henderson, B. W.; Jori, G.; Kessel, D.; Korbelik, M.; Moan, J.; Peng, Q. *J. Natl. Cancer Inst.* **1998**, *90*, 889−905. (b) Juzeniene, A.; Peng, Q.; Moan, J. *Photochem. Photobiol. Sci.* **2007**, *6*, 1234−1245. (c) Castano, A. P.; Demidova, T. N.; Hamblin, M. R. *Photodiagn. Photodyn. Ther.* **2004**, *1*, 279−293. (d) Castano, A. P.; Demidova, T. N.; Hamblin, M. R. *Photodiagn. Photodyn. Ther.* **2005**, *2*, 91−106.

(3) Plaetzer, K.; Krammer, B.; Berlanda, J.; Berr, F.; Klesslich, T. *Lasers Med. Sci.* **2009**, *24*, 259−268. M Detty, M. R.; Gibson, S. L.; Wagner, S. J. *J. Med. Chem.* **2004**, *47*, 3897−3915. Moan, J. *J. Photochem. Photobiol. B: Biol.* **1990**, *5*, 521−524.
(4) Moan, J. *J. Photochem. Photobiol. B: Biol.* **1990**, *6*, 343−344.
(5) (a) Oleinick, N. L.; Morris, R. L.; Belichenko, I. *Photochem. Photobiol. Sci.* **2002**, *1*, 1−21. (b) Fulda, S.; Galluzzi, L.; Kroemer, G. *Nature Rev. Drug Discovery* **2010**, *9*, 447−464. (c) Sasnauskiene, A.; Kadziauskas, J.; Veselyte, N.; Jonusiene, V.; Kirveliene, V. *Apoptosis* **2009**, *14*, 276−286. (d) Kessel, D.; Luo, Y. *Cell Death Differ.* **1999**, *6*, 28−35. (e) Green, D. R.; Reed, J. C. *Science* **1998**, *281*, 1309−1312.
(6) Johnson, L. V.; Walsh, M. L.; Chen, L. B. *Proc. Natl. Acad. Sci. U.S.A.* **1980**, *77*, 990−994.
(7) (a) Lee, D. R.; Helps, S. C.; Macardle, P. J.; Nilsson, M.; Sims, N. R. *Neurochem. Res.* **2009**, *34*, 1857−1866. (b) Ferlini, C.; Scambia, G. *Nat. Protocols* **2007**, *2*, 3111−3114. (c) Baracca, A.; Sgarbi, G.; Solaini, G.; Lenaz, G. *Biochim. Biophys. Acta—Bioenergy* **2003**, *1606*, 137−146.
(8) (a) Moreira, L. M.; dos Santos, F. V.; Lyon, J. P.; Maftoum-Costa, M.; Pacheco-Soares, C.; de Silva, N. S. *Aust. J. Chem.* **2008**, *61*, 741−754. (b) Miller, J. D.; Baron, E. D.; Scull, H.; Hsia, A.; Berlin, J. C.; McCormick, T.; Colussi, V.; Kenney, M. E.; Cooper, K. D.; Oleinick, N. L. *Toxicol. Appl. Pharmacol.* **2007**, *224*, 290−299. (c) Ogura, S.; Tabata, K.; Fukushima, K.; Kamachi, T.; Okura, I. *J. Porphyrins Phthalocyanines* **2006**, *10*, 1116−1124. (d) Lukyanets, E. A. *J. Porphyrins Phthalocyanines* **1999**, *3*, 424−432.
(9) (a) Longo, J. P. F.; Lozzi, S. P.; Simioni, A. R.; Morais, P. C.; Tedesco, A. C.; Azevedo, R. B. *J. Photochem. Photobiol. B: Biol.* **2009**, *94*, 143−146. (b) Vittar, N. B. R.; Prucca, C. G.; Strassert, C.; Awruch, J.; Rivarola, V. A. *Int. J. Biochem. Cell Biol.* **2008**, *40*, 2192−2205. (c) Derycke, A. S. L.; Kamuhabwa, A.; Gijsens, A.; Roskams, T.; de Vos, D.; Kasran, A.; Huwyler, J.; Missiaen, L.; de Witte, P. A. M. *J Natl. Cancer Inst.* **2004**, *96*, 1620−1630. (d) Qualls, M. M.; Thompson, D. H. *Int. J. Cancer* **2001**, *93*, 384−392. (e) Ginevra, F.; Biffanti, S.; Pagnan, A.; Biolo, R.; Reddi, E.; Jori, G. *Cancer Lett.* **1990**, *49*, 59−65.
(10) (a) Rijcken, C. J. F.; Hofman, J.-W.; van Zeeland, F.; Hennink, W. E.; van Nostrum, C. F. *J. Controlled Release* **2007**, *124*, 144−153. (b) Tailler, J.; Jones, M. C.; Brasseur, N.; van Lier, J. E.; Leroux, J. C. *J. Pharm. Sci.* **2000**, *89*, 52−62. (c) Foley, M. S. C.; Beeby, A.; Parker, A. W.; Bishop, S. M.; Phillips, D. *J. Photochem. Photobiol. B: Biol.* **1997**, *38*, 18−24.
(11) (a) Weider, M. E.; Hone, D. C.; Cook, M. J.; Handsley, M. M.; Gavrilovic, J.; Russell, D. A. *Photochem. Photobiol. Sci.* **2006**, *5*, 727−734. (b) Ricci-Junior, E.; Marchetti, J. M. *Int. J. Pharm.* **2006**, *310*, 187−195. (c) Ricci-Junior, E.; Marchetti, J. M. *J. Microencapsul.* **2006**, *23*, 523−538.
(12) (a) Kuznetsova, N. A.; Gretsova, N. S.; Derkacheva, V. M.; Kaliya, O. L.; Lukyanets, E. A. *J. Porphyrins Phthalocyanines* **2003**, *7*, 147−154. (b) Cauchon, N.; Tian, H.; Langlois, R.; La Madeleine, C.; Martin, S.; Ali, H.; Hunting, D.; van Lier, J. E. *Bioconjug. Chem.* **2005**, *16*, 80−89. (c) Kluson, P.; Drobek, M.; Kalaji, A.; Karaskova, M. *Res. Chem. Intermed.* **2009**, *35*, 103−116.
(13) (a) Kaliya, O. L.; Lukyanets, E. A.; Vorozhtsov, G. N. *J. Porphyrins Phthalocyanines* **1999**, *3*, 592−610. (b) Liu, W.; Jensen, T. J.; Fronczek, F. R.; Hammer, R. P.; Smith, K. M.; Vicente, M. G. H. *J. Med. Chem.* **2005**, *48*, 1033−1041. (c) Verdree, V. T.; Pakhomov, S.; Su, G.; Allen, M. W.; Countryman, A. C.; Hammer, R. P.; Soper, S. A. *J. Fluores.* **2007**, *17*, 547−563. (d) Ng, A. C. H.; Li, X.-Y.; Ng, D. K. P. *Macromolecules* **1999**, *32*, 5292−5298.
(14) Kuznetsova, N.; Makarov, D.; Yuzhakova, O.; Strizhakov, A.; Roumbal, Y.; Ulanova, L.; Krasnovsky, A.; Kaliya, O. *Photochem. Photobiol. Sci.* **2009**, *8*, 1724−1733.
(15) (a) Huang, J. D.; Wang, S. Q.; Lo, P. C.; Fong, W. P.; Ko, W. H.; Ng, D. K. P. *New J. Chem.* **2004**, *28*, 348−354. (b) Gijsens, A.; Derycke, A.; Missiaen, L.; de Vos, D.; Huwyler, J.; Eberle, A.; de Witte, P. *Int. J. Cancer* **2002**, *101*, 78−85. (c) Wohrle, D.; Muller, S.; Shopova, M.; Mantareva, V.; Spassova, G.; Vietri, F.; Ricchelli, F.; Jori, G. *J. Photochem. Photobiol. B: Biol.* **1999**, *50*, 124−128. (d) Egorin, M. J.; Zuhowski, E. G.; Sentz, D. L.; Dobson, J. M.; Callery, P. S.; Eiseman, J. L. *Cancer Chemother. Pharmacol.* **1999**, *44*, 283−294. (e) Allemann, E.; Rousseau, J.; Brasseur, N.; Kudrevich, S. V.; Lewis, K.; van Lier, J. E. *Int. J. Cancer* **1996**, *66*, 821−824.
(16) (a) Lo, P.-C.; Chan, C. M. H.; Liu, J.-Y.; Fong, W.-P.; Ng, D. K. P. *J. Med. Chem.* **2007**, *50*, 2100−2107. (b) Lo, P.-C.; Wang, S.; Zeug, A.; Meyer, M.; Roder, B.; Ng, D. K. P. *Tetrahed. Lett.* **2003**, *44*, 1967−1970.
(17) Ngen, E. J.; Rajaputra, P.; You, Y. *Bioorg. Med. Chem.* **2009**, *17*, 6631−6640.
(18) Derkacheva, V. M.; Mikhalenko, S. A.; Solov'eva, L. I.; Alekseeva, V. I.; Marinina, L. E.; Savina, L. P.; Butenin, A. V.; Luk'yanets, E. A. *Russ. J. Gen. Chem.* **2007**, *77*, 1117−1125.
(19) Kuznetsova, N.; Makarov, D.; Derkacheva, V.; Savvina, L.; Alekseeva, V.; Marinina, L.; Slivka, L.; Kaliya, O.; Lukyanets, E. *J. Photochem. Photobiol. A Chem.* **2008**, *200*, 161−168.
(20) Howe, L.; Zhang, J. Z. *J. Phys. Chem. A* **1997**, *101*, 3207−3213.
(21) Schmidt, R.; Afshari, E. *J. Phys. Chem.* **1990**, *94*, 4377−4378.
(22) Mak, N. K.; Li, K. M.; Leung, W. N.; Wong, R. N.; Huang, D. P.; Lung, M. L.; Lau, Y. K.; Chang, C. K. *Biochem. Pharmacol.* **2004**, *68*, 2387−2396.
(23) Ting, C. M.; Lee, Y. M.; Wong, C. K.; Wong, A. S.; Lung, H. L.; Lung, M. L.; Lo, K. W.; Wong, R. N.; Mak, N. K. *Biochem. Pharmacol.* **2010**, *79*, 825−841.
(24) Chan, P. S.; Koon, H. K.; Wu, Z. G.; Wong, R. N.; Lung, M. L.; Chang, C. K.; Mak, N. K. *Photochem. Photobiol.* **2009**, *85*, 1207−1217.
(25) Sheik-Bahae, M.; Said, A. A.; Wei, T.-H.; Hagan, D. J.; Van Stryland, E. W. *IEEE J. Quantum Electron.* **1990**, *26*, 760−769.
(26) Zhang, J; Wong, K.-L.; Wong, W.-K.; Mak, N.-K.; Kwong, W. J. D.; Tam, H. L. *Org. Biomol. Chem.* **2011**, DOI: 10.1039/c1ob05415e.
(27) Li, Y.; Pritchett, T. M.; Huang, J.; Ke, M.; Shao, P.; Sun, W. *J. Phys. Chem. A* **2008**, *112*, 7200−7207.
(28) *SAINT+*, version 6.02a; Bruker Analytical X-ray System, Inc., Madison, WI, 1998.
(29) Sheldrick, G. M. *SADABS, Empirical Absorption Correction Program*; University of Göttingen, Germany, 1997.
(30) Sheldrick, G. M. *SHELXTLTM, Reference Manual*, version 5.1; Bruker AXS, Inc.: Madison, WI, 1997.
(31) Bauer, H.; Stier, F.; Petry, C.; Knorr, A.; Stadler, C.; Staab, H. A. *Eur. J. Org. Chem.* **2001**, 3255−3278.
(32) Huang, J.-D.; Lo, P.-C.; Chen, Y.-M.; Lai, J. C.; Fong, W.-P.; Ng, D, K. P. *J. Inorg. Biochem.* **2006**, *100*, 946−951.
(33) Cammidge, A. N.; Nekelson, F.; Helliwell, M.; Heeney, M. J.; Cook, M. J. *J. Am. Chem. Soc.* **2005**, *127*, 16382−16383.
(34) Lo, P.-C.; Huang, J.-D.; Cheng, D. Y. Y.; Chan, E. Y. M.; Fong, W.-P.; Ko, W.-H.; Ng, D. K. P. *Chem.—Eur. J.* **2004**, *10*, 4831−4838.
(35) Zhao, Z.; Poon, C.-T.; Wong, W.-K.; Wong, W. Y.; Tam, H. L.; Cheah, K.-W.; Xie, T.; Wang, D. *Eur. J. Inorg. Chem.* **2008**, 119−128.
(36) Mak, N. K.; Li, K. M.; Leung, W. N.; Wong, R. N.; Huang, D. P.; Lung, M. L.; Lau, Y. K.; Chang, C. K. *Biochem. Pharmacol.* **2004**, *68*, 2387−2396.
(37) (a) Fredericksen, P. K.; Jorgensen, M.; Ogilby, P. R. *J. Am. Chem. Soc.* **2001**, *123*, 1215−1221. (b) Poulsen, T. D.; Fredericksen, P. K.; Jorgensen, M.; Mikkelsen, K. V.; Ogilby, P. R. *J. Phys. Chem. A* **2001**, *105*, 11488−11495. (c) Karotki, A.; Dorbizhev, M.; Kruk, M.; Spangler, C.; Nickel, E.; Mamar-Dashvili, N.; Rebane, A. *J. Opt. Soc. Am. B* **2003**, *20*, 321−332.
(38) Williams, R. M.; Piston, D. W.; Webb, W. W. *FASEB J.* **1994**, *8*, 804−813.
(39) Denk, W.; Strickler, J. H.; Webb, W. W. *Science* **1990**, *248*, 73−76.
(40) Ogawa, K.; Kobuke, Y. *Anti-Cancer Agents Med. Chem.* **2008**, *8*, 269−279.
(41) Xu, C.; Webb, W. W. *J. Opt. Soc. Am. B* **1996**, *13*, 481−491.
(42) Poon, C.-T.; Chan, P.-S.; Man, C.; Jiang, F.-L.; Wong, R. N. S.; Mak, N. K.; Kwong, D. W. J.; Tsao, S.-W.; Wong, W.-K. *J. Inorg. Biochem.* **2010**, *104*, 62−70.
(43) Saha, S.; Mallick, D; Majumdar, R.; Roy, M.; Dighe, R.; Jemmis, E.; Akhil, R.; Chakravarty, A. *Inorg. Chem.* **2011**, *50*, 2975−2987.